2.3 *Target Properties*

1. Radar Cross Section (RCS)
2. Swerling target fluctuation models
3. Bistatic equivalence theorem
4. Resonance scatter
5. Forward scatter
6. Glint mitigation

Radar Cross Section (RCS)

A formal definition of RCS is :

$$\sigma = \frac{\text{power reflected towards source/unit solid angle}}{\text{incident power density}/4\pi}$$

$$= \lim_{r \to \infty} 4\pi r^2 \left| \frac{E_r}{E_i} \right|^2$$

It depends on target dimensions (compared with the wavelength)
shape
materials
polarisation
:

Target Radar Cross Sections

Small, single engine aircraft	1 m^2
Jumbo jet	100
Small open boat	0.02
Frigate (1000 tons)	5,000
Truck	200
Car	100
Bicycle	2
Person	1
Bird	0.01
Insect	10^{-5}

Adapted from M.I. Skolnik, *Introduction to Radar Systems*, 1962 (first edition).

RCS of sphere

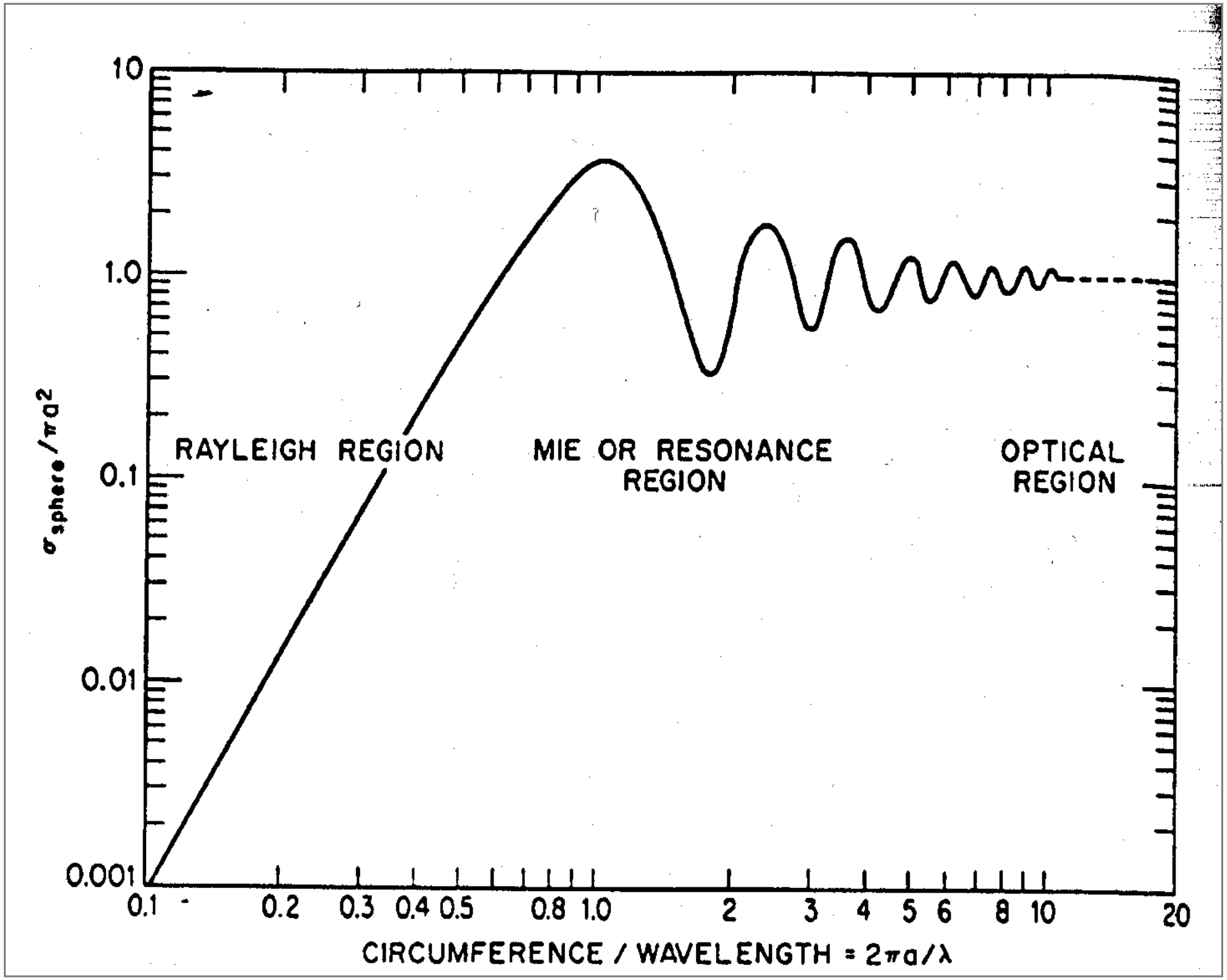

Test your understanding

Why is the sky blue ?

And why is the sunset red ?

RCS of flat plate

Assume a perfectly-conducting square plate, of side *a* (large compared to wavelength), with signal at normal incidence

power intercepted in power density of Φ W/m^2 $= \Phi . a^2$ Watts

This is reradiated as though from a uniform aperture of side *a*, i.e. with a radiation pattern

$$E(\theta) = \frac{\sin\left[\pi(a/\lambda)\sin\theta\right]}{\pi(a/\lambda)\sin\theta}$$

and with a gain normal to the surface of $\dfrac{4\pi a^2}{\lambda^2}$

i.e. $$P_r = \frac{P_t G_t}{4\pi r^2} . \underbrace{a^2 . \frac{4\pi a^2}{\lambda^2}}_{\sigma} . \frac{1}{4\pi r^2} . \frac{G_r \lambda^2}{4\pi}$$

so the RCS is $\sigma = \dfrac{4\pi a^4}{\lambda^2}$ or in general, for a plate of area *A*, $\sigma = \dfrac{4\pi A^2}{\lambda^2}$

Practical targets

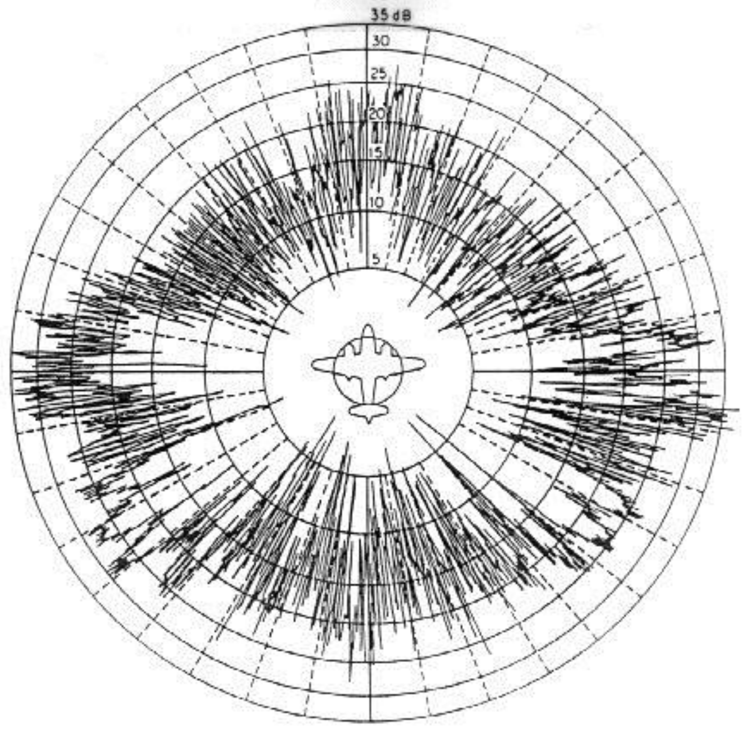

Figure 3.1 Measured azimuthal pattern of the radar backscatter from a B-26 airplane at 10-cm wavelength. (From Ridenour [103], courtesy McGraw-Hill Book Company).

The RCS of practical targets depends strongly on aspect angle

Target echo fluctuations

The analysis of detection has so far assumed that the echo signal from a given target is constant. In practice, real targets are made up of several scatterers, and the net echo depends on the way in which the contributions from these scatterers add vectorially, and the way in which the motion of the target (and/or radar) cause the sum to vary from pulse to pulse and scan to scan.

The effect was studied by Swerling, who defined four cases of target echo fluctuation, and these have been widely used.

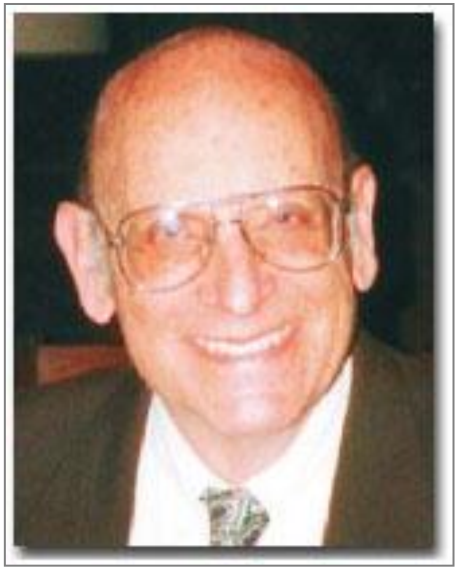

Swerling target fluctuation models

Swerling 0: echo pulses are constant from pulse to pulse and scan to scan.

Swerling 1: echo pulses are assumed to be be correlated (of constant amplitude) from pulse to pulse, but uncorrelated (independent) from scan to scan. Scan to scan fluctuations are described by an exponential pdf:

$$p(\sigma) = \frac{1}{\sigma_{av}} \exp\left(-\frac{\sigma}{\sigma_{av}} \right) \qquad \sigma \geq 0$$

Swerling 2: echo pulses are uncorrelated from pulse to pulse (and therefore also from scan to scan). The pulse to pulse fluctuations are described by the same exponential pdf as for Swerling 1 targets.

Swerling 3: Swerling 1 and 2 evidently correspond to cases where the target is composed of a large number of similar scatterers, and hence where Gaussian statistics apply. We can also have targets where there is one dominant scatterer plus a number of other smaller scatterers. In such a case:

$$p(\sigma) = \frac{4\sigma}{\sigma_{av}^2} \exp\left(-\frac{2\sigma}{\sigma_{av}} \right)$$

A Swerling 3 target is one whose RCS is constant from pulse to pulse, but whose scan to scan fluctuations obey this equation.

Swerling 4: echo pulses are uncorrelated from pulse to pulse (and therefore also from scan to scan), and the pulse to pulse variations obey this equation.

Bistatic RCS: the equivalence theorem

The bistatic RCS is equal to the monostatic RCS at the bisector of the bistatic angle β, reduced in frequency by the factor $\cos(\beta/2)$, given:

- sufficiently smooth targets
- no shadowing
- retroreflectors persist

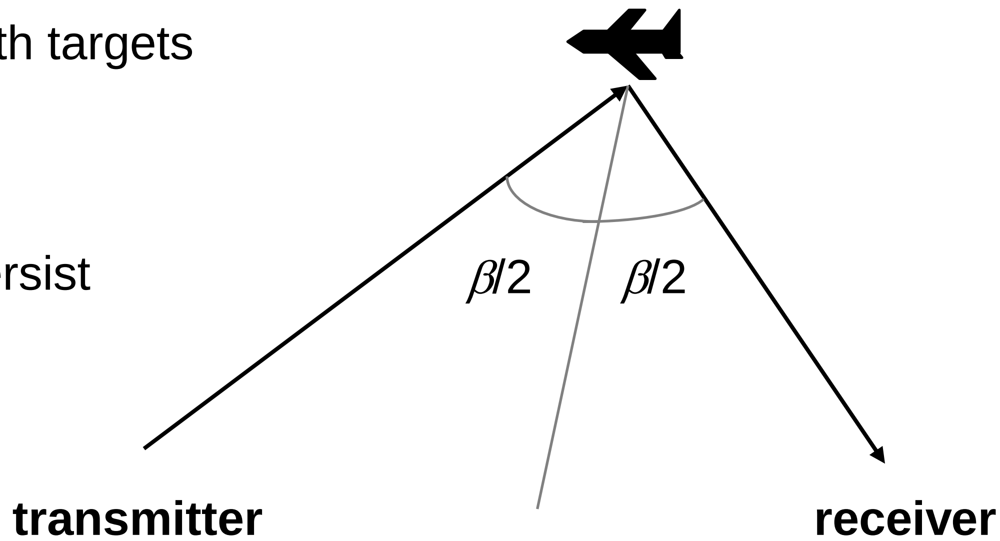

Crispin, J.W., Goodrich, R.F. and Siegel, K.M., 'A theoretical method for the calculation of the radar cross-sections of aircraft and missiles', University of Michigan, report 2591-1-1-M, AF 19(604)-1949, AFCRC-TN-59-774, 1959.

Kell, R.E., 'On the derivation of bistatic RCS from monostatic measurements', *Proc. IEEE*, Vol.53, pp983-988, 1965.

Bistatic RCS

Three bistatic RCS phenomena that may be exploited as a counter to stealth aircraft have been identified:

- resonance scatter
- forward scatter
- specular reflection

Resonance scatter and specular reflection apply also to monostatic radar; forward scatter applies only to bistatic radar.

Resonance scatter

- The resonance scatter effect for monostatic radars has been well documented for conventional (non-stealth) targets. In the simplest case of a conducting sphere of radius *a*, resonance occurs in the region 0.5 < $2\pi a/\lambda$ < 10.
- "Physically, the resonant region can be explained by the interference between the incident wave and the creeping wave, which circles the sphere and either adds to or subtracts from the total field at the leading surface" (Barton)

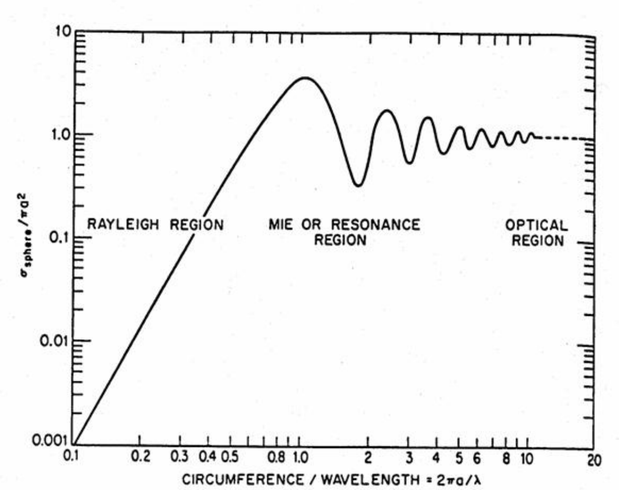

- The net result of these additive effects is that when wavelengths are of the order of discrete aircraft dimensions, for example fuselage, wing, tail, inlet and exhaust ducts, the resulting resonance significantly enhances RCS when compared to the optical region, which for the sphere starts at $2\pi a/\lambda$ >10.

Resonance scatter

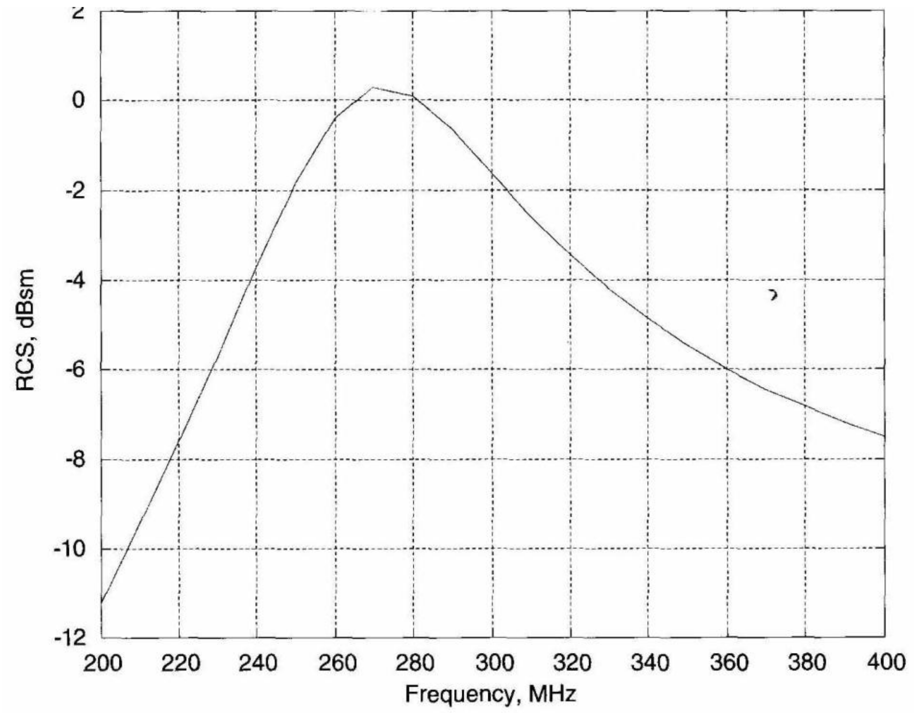

Monostatic radar cross section of a simple, wire-grid aircraft model using method-of-moments computed patterns, TE-polarized incident plane wave. The peak in the curve around 270 MHz is due to a resonance condition for the fuselage. Resonances occur at several frequencies due to various aircraft parts and are most pronounced for slender metallic shapes. The resonance effect for this model ends at about 400 MHz. Courtesy AIAA.

David C. Jenn, *Radar and Laser Cross Section Engineering, 2nd Ed.,* AIAA Education Series, Reston, VA 2005.

Resonance scatter

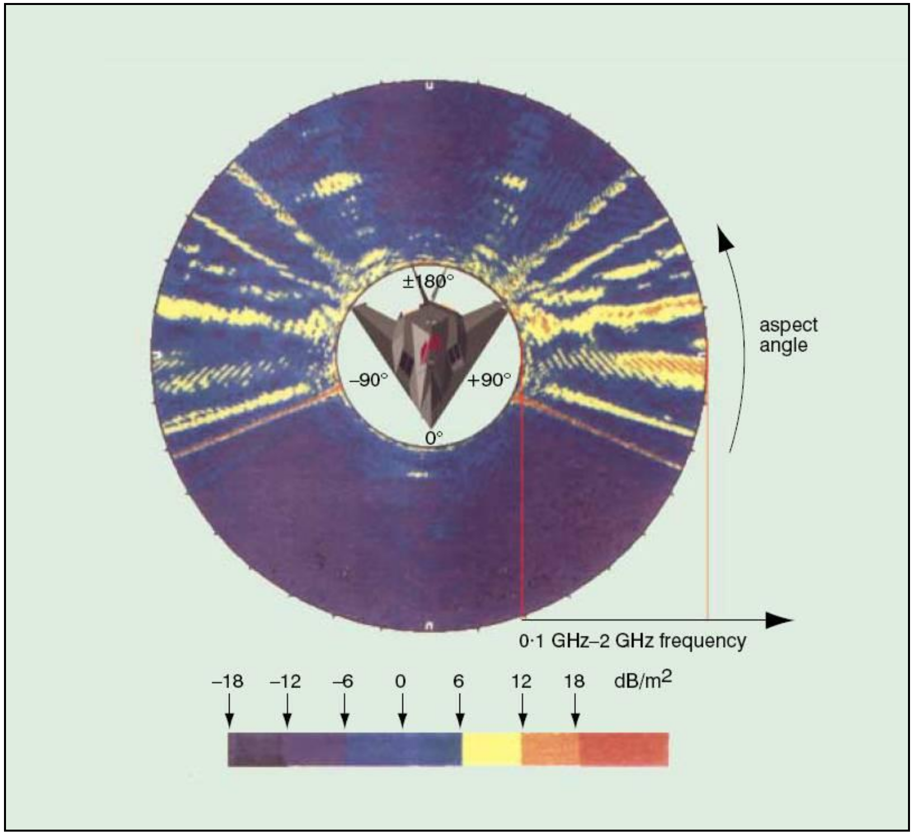

Deutsche Aerospace, Bremen anechoic chamber measurements of a faceted, metallized 1:10 scale model of an F-117 aircraft:

"The aircraft geometry was obtained from open literature and hence the target model does not take into account fine structure details and surface materials such as RAM, which are of less importance at VHF/UHF…"

"The scaled measurement results… show that the attempt to reduce the target's RCS has been successful in the ± 70º section around the nose-on aspect and for the frequency range above 400 MHz. High RCS values covering the whole frequency range occur when the direction of illumination is perpendicular to the front or back edges of the wings or other dominant structures of the fuselage. In the nose-on section, however, an increase in the RCS can be seen at VHF around 100 MHz [6 to10 dBm^2] and UHF around 400 MHz [0 to 6 dBm^2, > 6 dBm^2 nose on] due to resonance effects. Hence, such stealth techniques can be efficient at high radar frequencies but are ineffective at VHF/UHF."

Kuschel, H., 'VHF/UHF radar, part 1: characteristics; part 2: operational aspects and applications', *Electronics and Communications Journal,* Vol.14, No.2, pp 61-72, April 2002, and Vol.14, No.3, pp 101-111, June 2002.

Forward scatter

Babinet's principle tells us that we get exactly the same scattering from a perfectly-absorbing target as we would from a target-shaped hole in an infinite perfectly-conducting sheet !

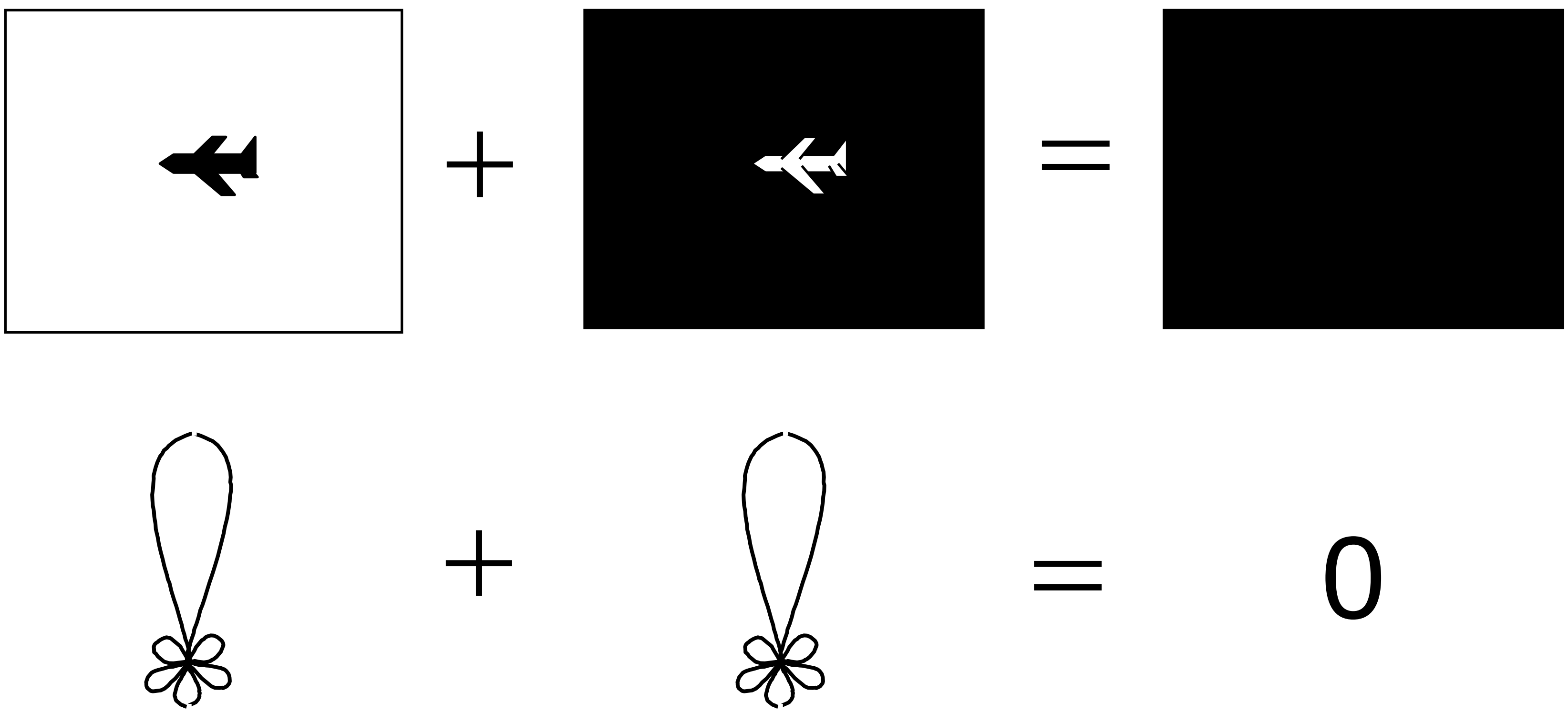

Forward scatter

So a target on the transmitter-receiver baseline, even if it is completely stealthy, will scatter a significant amount of energy - in fact the RCS will be of the order of

$$\sigma_b = \frac{4\pi A^2}{\lambda^2}$$

The angular width of the scattering will be of the order of

$$\frac{\lambda}{d} \quad \text{(radians)}$$

which tends to favour a low frequency.

Forward scatter

$$\sigma_b = \frac{4\pi A^2}{\lambda^2}$$

$$\theta_B \approx \frac{\lambda}{d} \quad \text{(radians)}$$

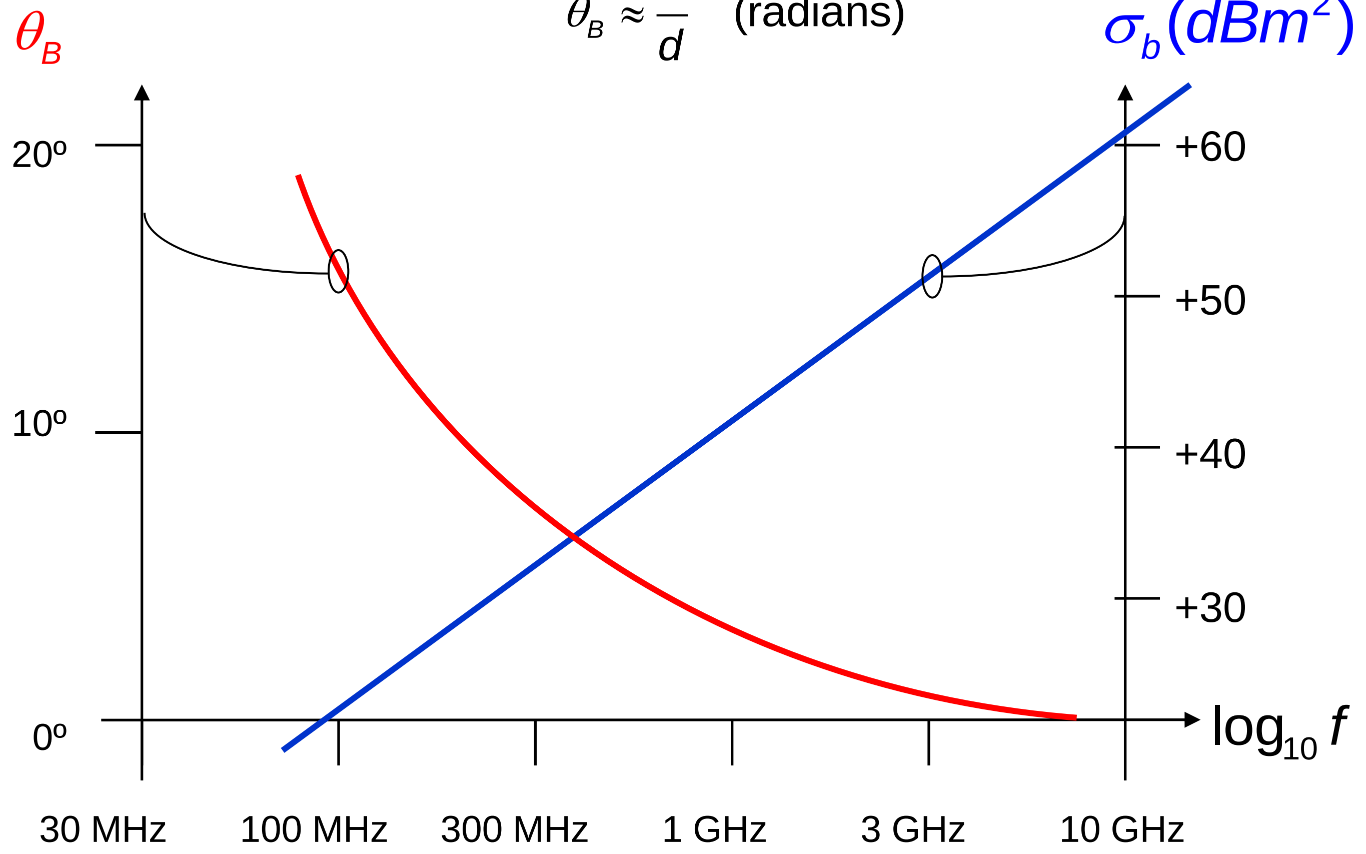

Forward scatter

<u>But</u> a target which lies exactly on the transmitter-receiver baseline will give no range information and no Doppler information, and even for a target only slightly off-baseline the range and Doppler resolution will be poor

So whilst a forward scatter radar will be good for target detection, location and tracking will be more difficult.

As well as that, the clutter RCS will be high, both because of the large clutter cell area and because the clutter scattering coefficient ($\sigma°$) will be high. Detection is therefore likely to be clutter-limited rather than noise-limited.

Forward scatter fences

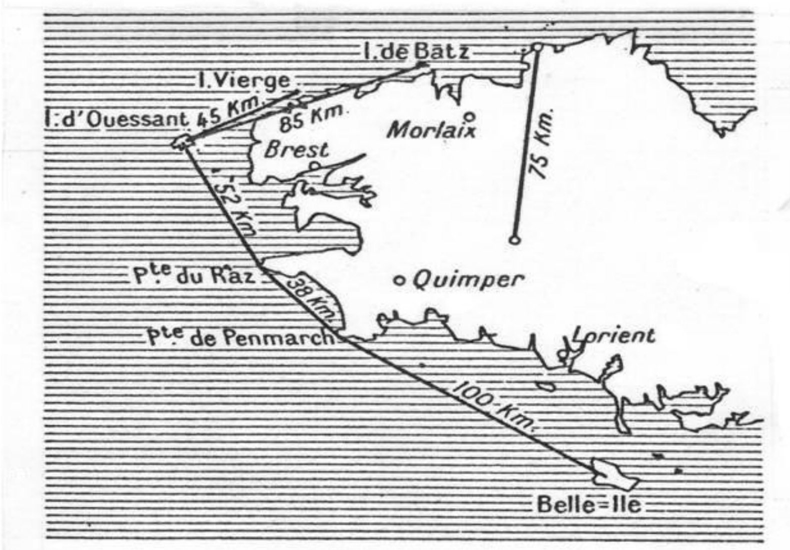

Fig. 1. — « Barrages électromagnétiques » protégeant Brest en 1939

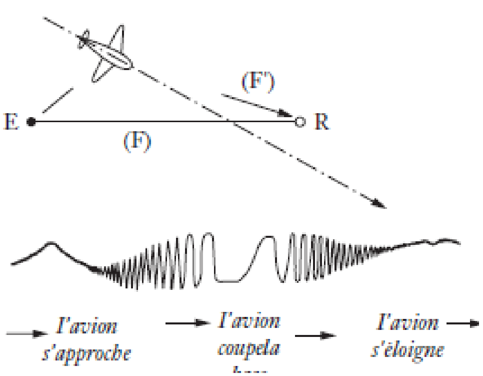

Six of Pierre David's 30 MHz radar fences deployed around Brest in 1939 – also around Cherbourg, Toulon and Bizerte (Tunisia).

It is not clear why two gaps remained. Note the near parallel fences in the northwest coverage, which suggest partial elements of his more complex configuration called the *maille en Z*. It could generate course and speed estimates for non-manoeuvering aircraft.

Pierre David, *Le Radar*, PUK Coll. Que sais-je? No. 381, 1969.

Iso-phase contours

each contour represents an extra wavelength in the transmitter-target-receiver path

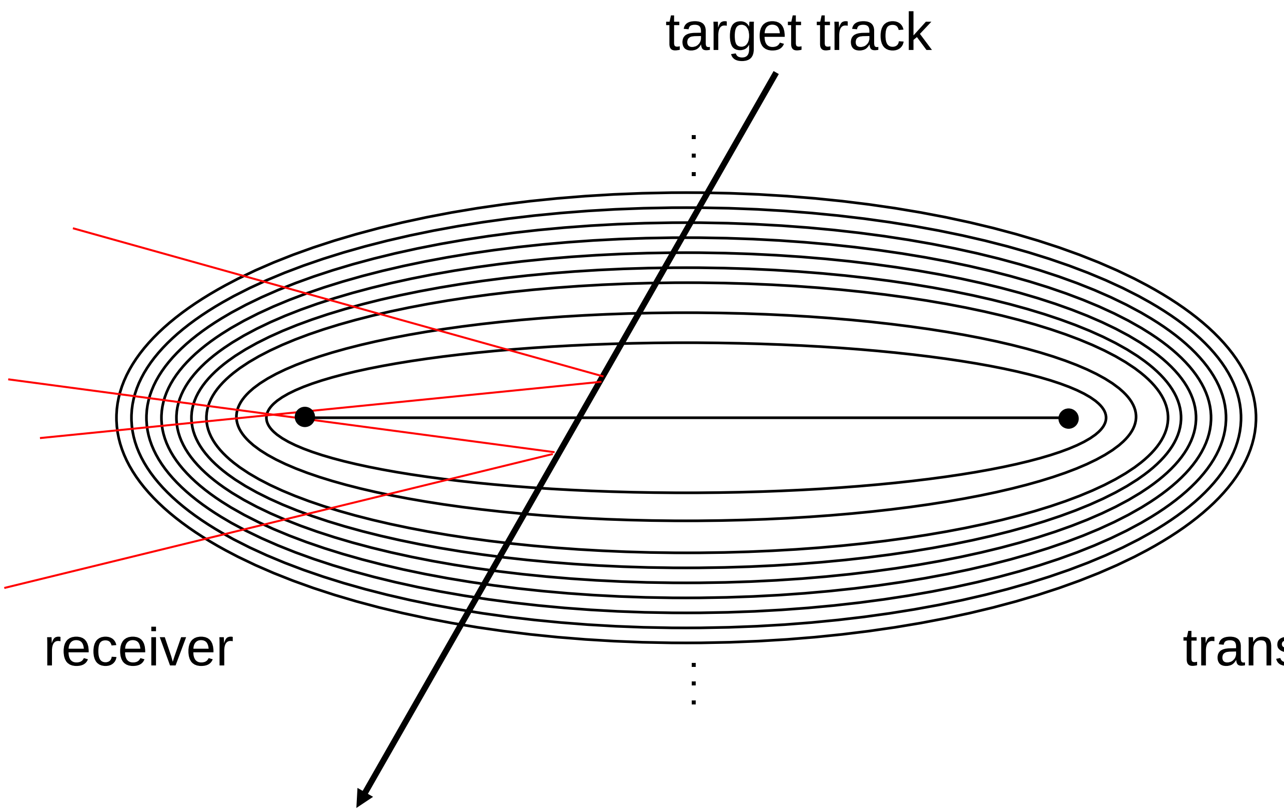

Specular reflection

- A third counter-stealth capability has sometimes been ascribed to bistatic radars in general: the ability to detect specular reflections that have purposely been directed away from anticipated monostatic radar threat locations, for example by using tilted surfaces or facets on stealth platforms.
- The assertion is that through judicious location of multiple bistatic receivers, these off-normal speculars of large amplitude can be detected and tracked or networked together to support some level of engagement.
- However, this requires rather specific geometries, and the flashes will be of short duration, so at this time it would appear optimistic to ascribe more than a fence-type alerting and coarse cueing capability when exploiting specular reflections from stealth aircraft.

Bistatic/Monostatic RCS ratios for 4 small freighters X-band, grazing incidence

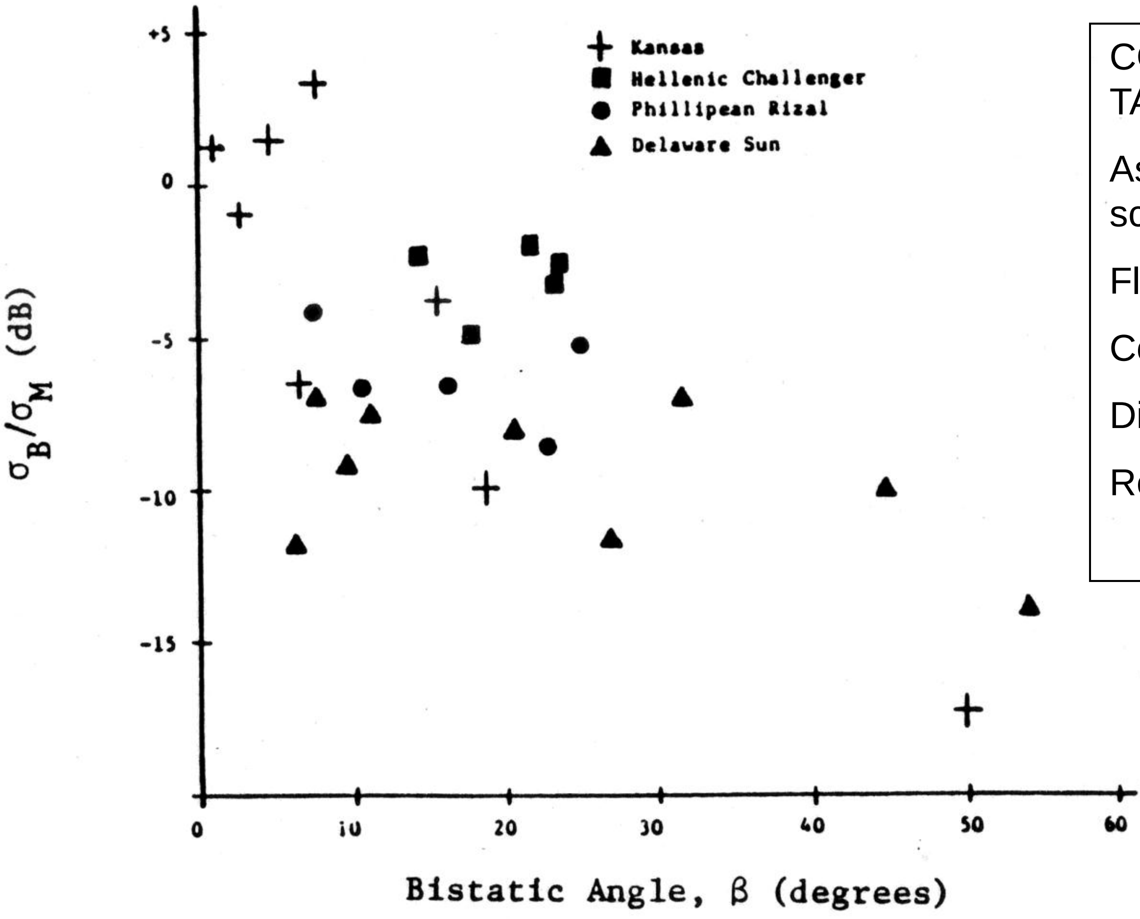

COMPLEX TARGETS:

Assembly of discrete scattering centers

Flat plates

Corner reflectors

Dihedrals

Resonant cavities

Ewell, G.W. and Zehner, S.P., 'Bistatic radar cross section of ship targets', *IEEE J. Oceanic Engineering*, Vol.OE-5, No.4, pp211-215, October 1980.

Radar glint mitigation
for semiactive homing missiles

- **DEFINITION OF GLINT**

  Angular displacement of the apparent phase centre of a target return at the missile's seeker

- **CAUSE**

  Phase interference between two or more dominant target scatterers lying within the seeker's resolution cell

- **EFFECT**

  As the target aspect angle changes, the apparent phase centre changes, increasing seeker angle tracking errors and thus miss distance

- **TYPICAL MITIGATION**

  Reduce size of resolution cell

  Smooth returns via non-coherent integration

  Operate bistatically

Monostatic and bistatic yaw plane glint

NOTES

Glint is modeled ± 60º off port broadside

Phase center is at the end of each line

Displacement is significantly reduced for β > ~15 º

Hence angle tracking is improved and miss distance is reduced

[Complex target → Smooth(er) target]

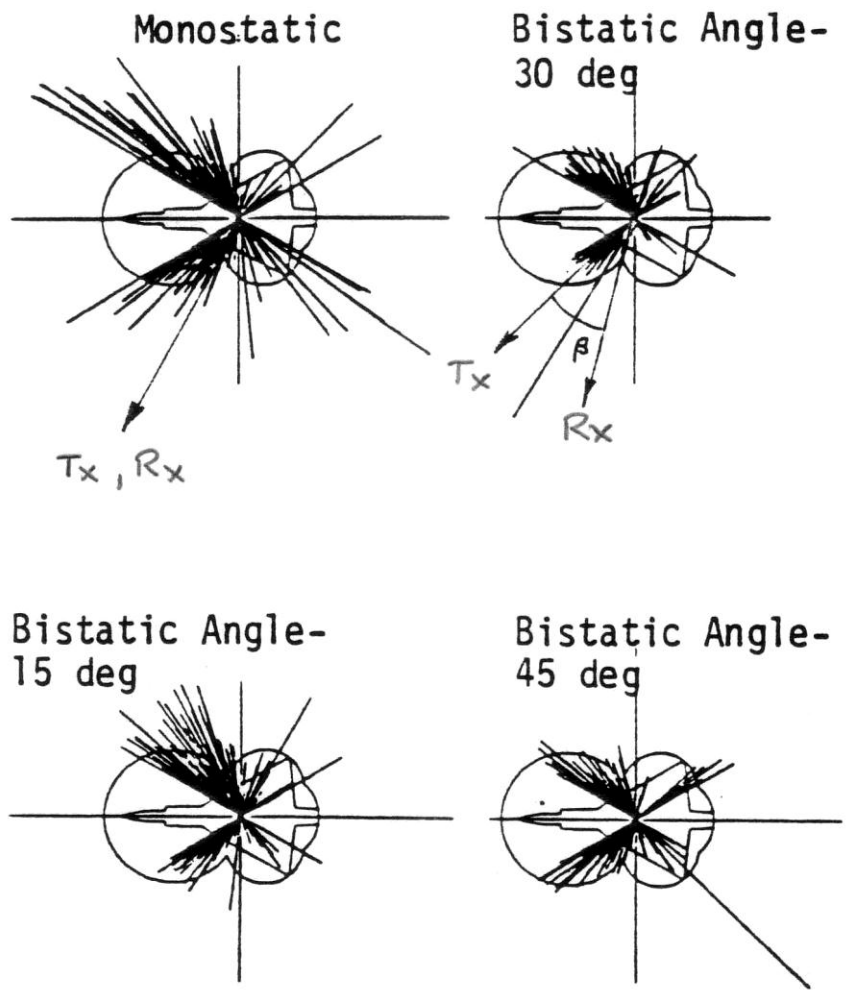

Group Exercise

In measurements of targets and clutter, it is desirable to calibrate the measurements against some sort of calibration target of known RCS. The choice of calibration target is a compromise between accuracy of RCS, ease of deployment, magnitude of RCS vs physical size, and cost.

For monostatic measurements a trihedral corner reflector is often used, since this has an RCS that is largely independent of aspect angle, but this is not so useful for bistatic measurements.

So can you compare the properties of different types of calibration target that might be used for bistatic measurements ? You might like to consider:

- trihedral corner reflector
- flat metal plate
- van Atta array
- transponder
- metallised sphere

:

RCS of sphere

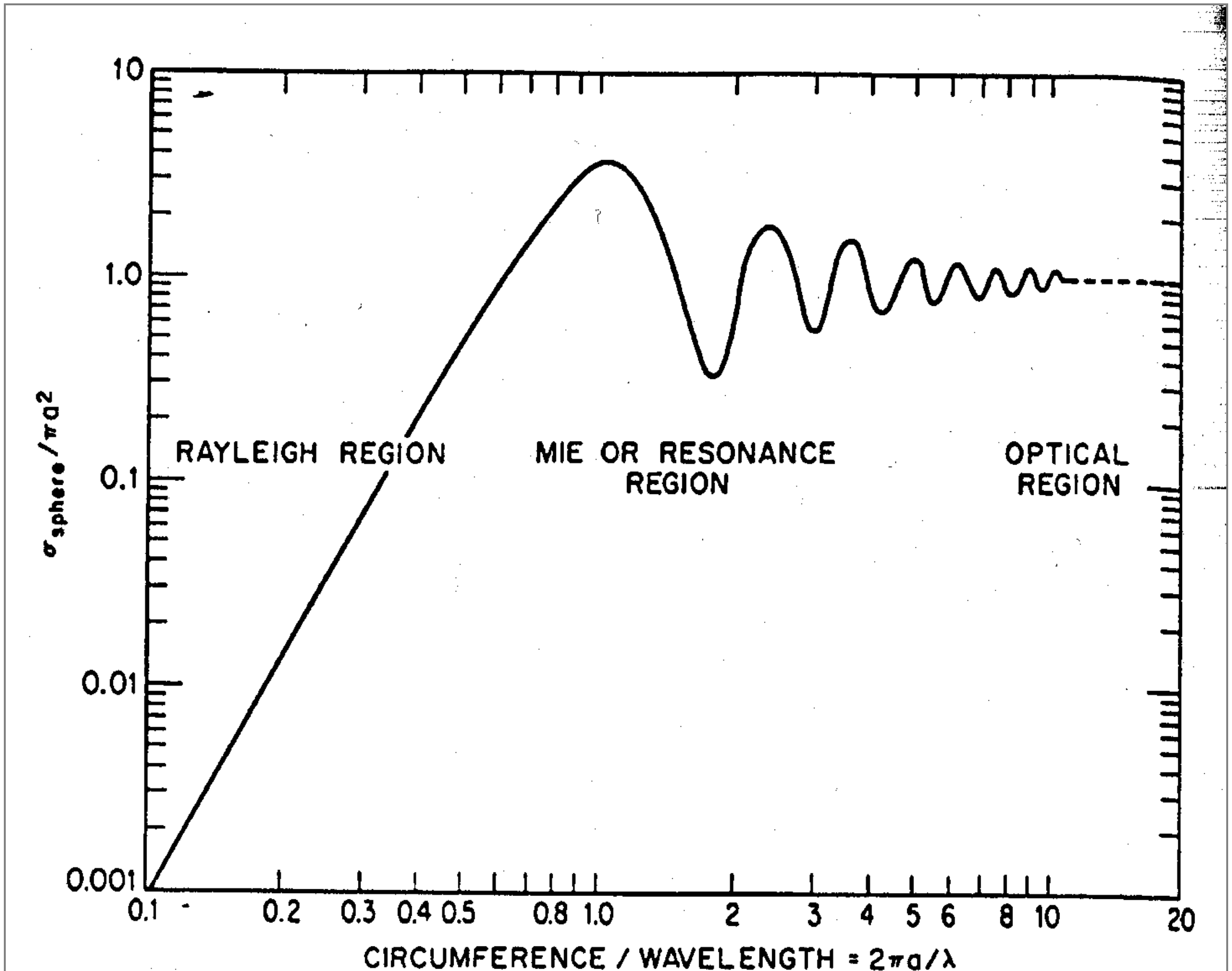

Sphere calibration target

RCS of flat plate

Assume a perfectly-conducting square plate, of side *a* (large compared to wavelength), with signal at normal incidence

power intercepted in power density of Φ W/m^2 $= \Phi \, . \, a^2$ Watts

This is reradiated as though from a uniform aperture of side *a*, i.e. with a radiation pattern

$$E(\theta) = \frac{\sin\left[\pi (a/\lambda) \sin\theta\right]}{\pi (a/\lambda) \sin\theta}$$

and with a gain normal to the surface of $\dfrac{4\pi a^2}{\lambda^2}$

i.e. $$P_r = \frac{P_t G_t}{4\pi r^2} . \underbrace{a^2 . \frac{4\pi a^2}{\lambda^2}}_{\sigma} . \frac{1}{4\pi r^2} . \frac{G_r \lambda^2}{4\pi}$$

so the RCS is $\sigma = \dfrac{4\pi a^4}{\lambda^2}$ or in general, for a plate of area *A*, $\sigma = \dfrac{4\pi A^2}{\lambda^2}$

Dihedral and trihedral corner reflectors

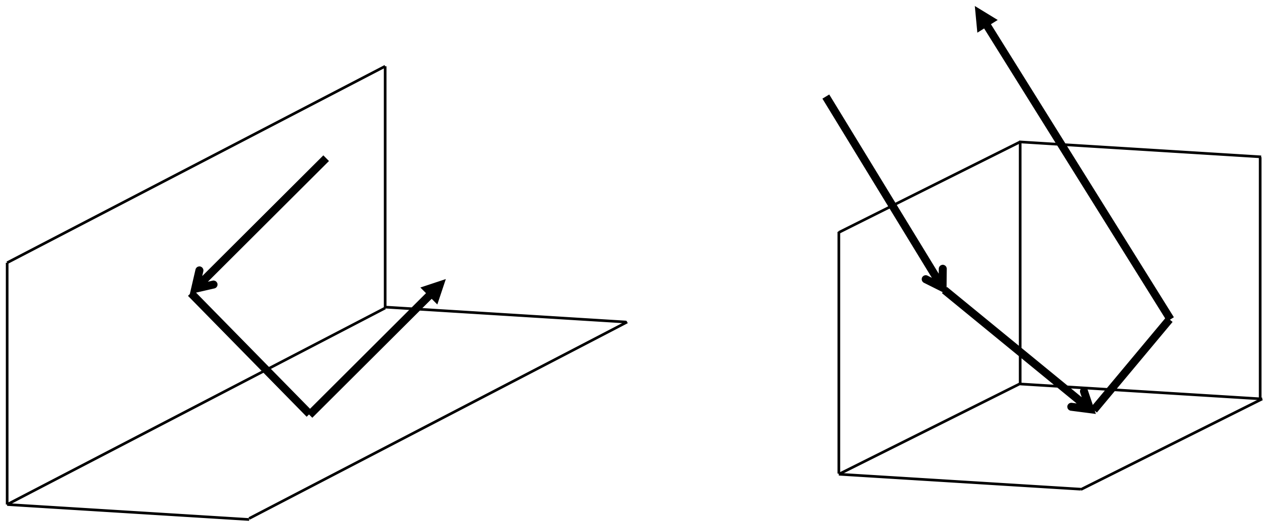

Trihedral corner reflector

Trihedral corner reflector

Luneberg lens

$$n(\rho) = \sqrt{2 - \frac{\rho^2}{R^2}}$$

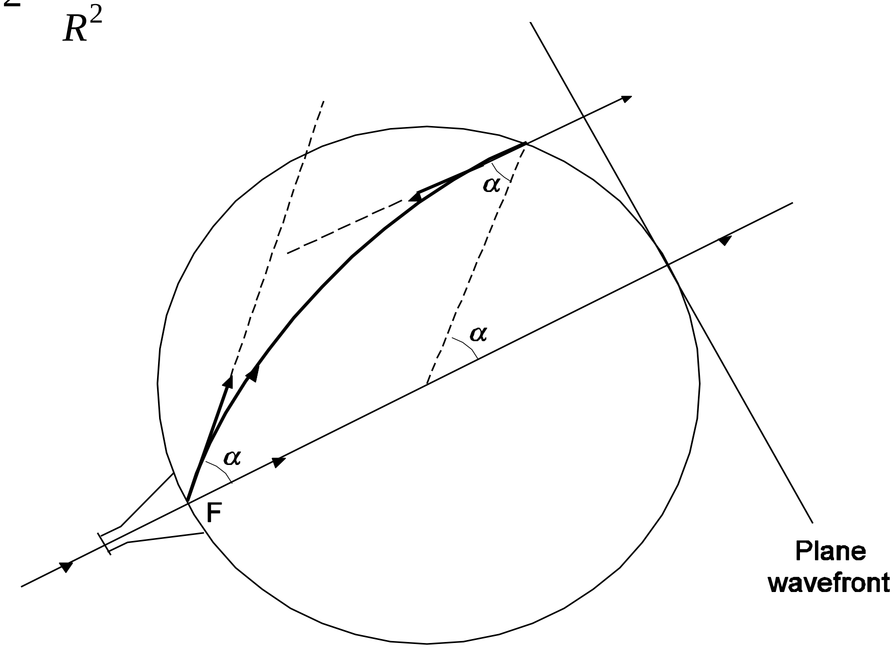

Van Atta arrays

Another approach is provided by the Van Atta array, which may be regarded as the passive array equivalent of the corner reflector. Elements equally displaced from the centre of the array are connected by equal length transmission lines; thus the signal received at each element is reradiated from its counterpart with a phase such that a beam is formed in the direction of the incident signal.

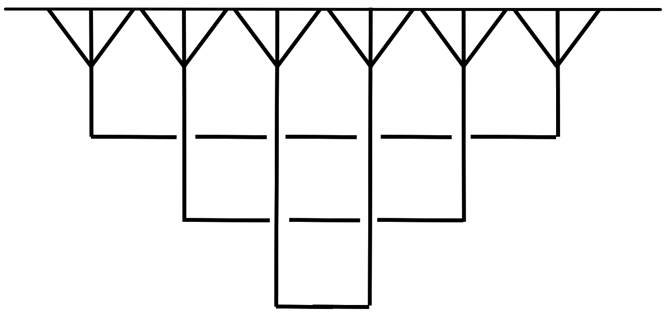

The retrodirective array will work over a range of directions determined by the beamwidths of the individual elements, which can in principle cover a broad range of angles. The basic idea can readily be extended to a planar array.

An *n*-element Van Atta array has a maximum RCS (in the absence of losses) of

$$\sigma = \frac{n^2 G_e^2 \lambda^2}{4\pi}$$

Van Atta arrays

The effective RCS can be increased by including bidirectional amplifiers in each path; however, the gain of the amplifiers must not exceed the combined isolation of the circulators (or, indeed, the coupling between corresponding elements) or instability will result. For the same reason, it is important that the elements present a good impedance match.

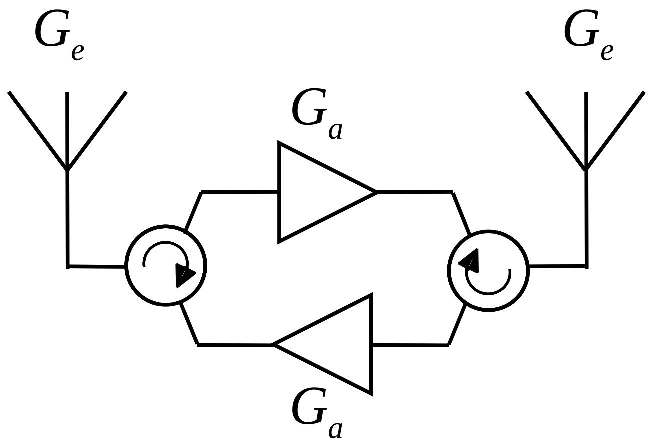

The maximum RCS of the arrangement is $\sigma = \dfrac{n^2 G_e^2 G_a \lambda^2}{4\pi}$

Summary

- The Bistatic Equivalence Theorem can be used to predict a target's bistatic RCS from its monostatic RCS – but beware of its assumptions and limitations
- The radar signature of a target can be substantially increased in forward scatter, even for a stealthy target
- Targets with dihedral or trihedral features will exhibit a higher monostatic RCS than bistatic.
- Glint may be significantly reduced in the bistatic configuration